Petrology of the late-Carboniferous Punta Falcone gabbroic complex, Northern Sardinia, Italy

Contrib Mineral Petrol (1992) 110:16–32

Contributions to Mineralogy and Petrology

Petrology of the late-Carboniferous Punta Falcone gabbroic complex, northern Sardinia, Italy

Simone Tommasini and Giampiero Poli

Dipartimento di Scienze della Terra, Piazza Universitá, I-06100 Perugia, Italy

Received February 13, 1991/Accepted July 21, 1991

Abstract. The Punta Falcone gabbroic complex represents an evolved high-alumina basalt which rose from the mantle through the lower crust, and subsequently intruded a granite magma in middle crustal levels, during the calc-alkaline magmatic activity which took place in the Sardinian and Corsican islands in the Carboniferous. The gabbroic complex has a stratified sub-vertical structure, and consists of three zones developing from the bottom to the top of the magma chamber. An interaction zone can be recognized along contacts with the surrounding granite stock, and it is characterized by finer-grained and more evolved rocks than the interior of the gabbroic complex. Processes occurring in its interior zone have been substantially different from those occurring in its marginal interaction zone. Petrographical and geochemical features indicate that the differentiation of the interior of the gabbroic complex can be accounted for by low pressure, closed-system in-situ crystallization. The different gabbroic units represent mixtures between cumulus phases and trapped liquid. Plagioclase + pyroxenes, and successively plagioclase + calcic amphibole + oxides nucleated and grew in-situ on the floor and walls of the chamber. Floating of plagioclase towards the top of the magma chamber resulted in the accumulation of the denser liquid at the bottom. Compaction phenomena and convective fractionation processes permitted the development of the pile of cumulus crystals with their trapped liquid, and the migration of part of this evolved liquid towards the top of the magma chamber. On the basis of major and trace element modelling a mathematical artifice has been developed to evaluate cumulus-intercumulus processes that occurred in the interior of the gabbroic complex. Accordingly, the formation of the different units can be modelled by mixtures between the parental magma and different percentages of minerals formed during the first stages of crystallization. Contemporaneously with the differentiation of the interior zone, the envelope of fine-grained rocks enclosing and grading into the coarser inner part of the gabbroic complex experienced both chemical and physical processes. Chemical processes resulted in the evolution of the marginal interaction zone by crystal fractionation plus contamination by the acid magma. Physical processes were closely related to the thermodynamic instability of this marginal zone, and consisted of mingling and back veining phenomena which developed interdigitations of granite veins along contacts. In addition, an increase of the melt fraction of the granite magma, superheated by the latent heat of crystallization of the mafic magma, caused the occurrence of tilting of the mafic magma chamber, and resulted in the development of the sub-vertical structure of the gabbroic complex.

Introduction

Studies of layered mafic intrusions can provide important constraints on the crystallization and chemical evolution of magma chambers. Nevertheless, one of the main problems dealing with layered mafic intrusions is that liquid compositions are not directly available and can only be estimated by either the chilled margin method (e.g. Wager and Brown 1967) or the weighted summation method (e.g. Ragland and Butler 1972; Klewin 1990). Moreover, processes such as open-system crystallization, convection, crystal sorting, and subsolidus re-equilibration make the scenario more complicated (e.g. Irvine 1979, 1980). Thus, the differentiation processes of most layered intrusions are still a matter of debate (e.g. Skaergaard: Hunter and Sparks 1987, 1990; McBirney and Naslund 1990; Morse 1990; Brooks and Nielsen 1990).

This paper is an attempt to explain differentiation processes that operated in a small (0.2 km^2), layered, mafic intrusion outcropping in Northern Sardinia (Italy), which intruded a still partially molten granite magma. The co-existence of partially molten magmas of different composition also offers the opportunity to study interaction processes occurring between crustal- and mantle-derived magmas in calc-alkaline plutonic environments.

Geology

The Punta Falcone gabbroic complex represents a globule of mafic magma (0.2 km^2, Fig. 1) injected into a granitic magma during the

calc-alkaline magmatic activity which took place in the Carboniferous and formed the Sardinia-Corsica batholith (Orsini 1980; Bralia et al. 1982; Poli et al. 1989).

Three zones can be recognized in the gabbroic complex passing from the western to the eastern edge, i.e. from the bottom to the top of the magma chamber (Fig. 2). The Lower Zone (LZ) is composed of granular, medium-grained gabbros (LZ-Ga) bearing plagioclase and calcic amphiboles as main phases, and clinopyroxene, oxides, biotite, and quartz in subordinate amounts. The Middle Zone (MZ) is composed of medium-grained leucogabbros (MZ-Lga) which mainly display orthocumulate textures, with plagioclase and tschermakite as cumulus and intercumulus phase, respectively. Clinopyroxene, biotite, oxides, and quartz occur as minor phases. This unit locally exhibits microrhythmic, mineral-graded layering (3-4 cm) consisting of plagioclase and ferroan pargasitic hornblende laminae. The layering dips steeply 70–80° east northeast. A lens of gabbros (MZ-Ga), with plagioclase and orthopyroxene as cumulus phases and large oikocrysts (up to 2cm) of pargasite and ferroan pargasitic hornblende occurs within the MZ-Lga (Fig. 1). Clinopyroxene, oxides, biotite, and quartz are minor phases. The widespread presence of fibrous amphibole belonging to the cummingtonite-grunerite series is also worth noting. This type of amphibole occurs in large amounts in this unit (up to 20 vol%) and is found replacing orthopyroxene. The Upper Zone (UZ) is composed of granular, medium- to fine-grained quartz-gabbros (UZ-Qga) bearing plagioclase, calcic amphiboles, biotite, and quartz as main phases, and clinopyroxene, oxides, and K-feldspar as minor phases. Two lenses of gabbros (UZ-Ga) which have textural and petrographical characteristics similar to the LZ-Ga occur within the UZ-Qga (Fig. 1).

In addition, a 2 m thick Interaction Zone (IZ) can be recognized along contacts with the surrounding granite stock. It is composed of fine-grained rocks ranging in composition from quartz-gabbros and diorites, to tonalites and granodiorites, outcropping in the western and eastern edge, respectively. Small outcrops of the IZ are also present both at the topographic top of the MZ and UZ, and as detached, dike-like fragments in the surrounding granite at the northwestern edge of the gabbroic complex (Fig. 1). The IZ rocks show a wide variability in modal compositon and consist of plagioclase, calcic amphibole, biotite, oxides, K-feldspar, and quartz. They locally exhibit porphyritic textures because of large plagioclase xenocrysts (up to 1 cm) inherited from the granite magma; poikilitic crystals of quartz and perthitic K-feldspar enclosing calcic amphibole, plagioclase, and biotite are also common. Angular fragments ($\sim 20 \times 30$ cm) of the different gabbroic units are locally found within the IZ rocks. Dense interdigitations of granite veins, joined with extensive mingling processes, occur in the eastern IZ, whereas they are absent in the western IZ.

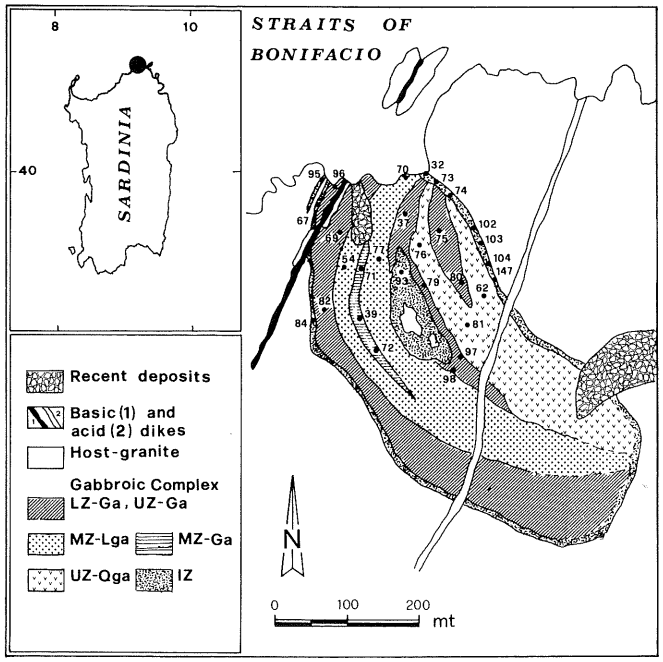

Fig. 1. Geological map of the Punta Falcone gabbroic complex, Northern Sardinia, Italy, and location of samples

Mineralogy

Compositions of the minerals in polished thin sections have been determined with an ARL-SEMQ wavelength dispersive electron microprobe using the analytical scheme by Colby (1971). Operating conditions were 15 KeV, 20 nA beam current, and a counting time varying from 10 to 20 s. In Tables 1, 2, 3, and 4 representative analyses of the main mineral phases are reported. The complete data set is available from the authors on request.

Plagioclase is the most important mineral phase in the Punta Falcone gabbroic complex. It always occurs as euhedral, lath-shaped, and subhedral grains with fairly constant core composition. In the MZ units plagioclase is the main cumulus phase: the crystals of the MZ-Lga display a normal zoning (core An_{90-85}, rim An_{60-51}), whereas those of the MZ-Ga are unzoned (An_{90-87}). Composition of plagioclase in LZ-Ga, UZ-Ga, and UZ-Qga is core An_{90-80} and rim An_{55-39}. In the IZ, single plagioclase crystals are unzoned, even though they show a compositional range from An_{70} to An_{23}; the most anorthite-rich plagioclases occur in the western IZ. Patchy

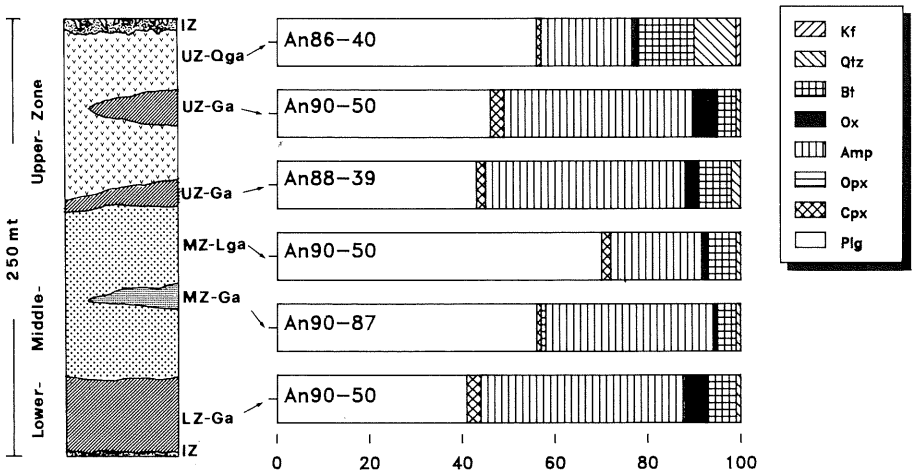

Fig. 2. Stratigraphic column of the Punta Falcone gabbroic complex, and average modal composition of the main units. Kf, K-feldspar; Qtz, quartz; Bt, biotite; Ox, oxides; Amp, magmatic and reaction amphiboles (see text); Opx, orthopyroxene; Cpx, clinopyroxene; Plg, plagioclase

Table 1. Selected plagioclase analysis, Punta Falcone gabbroic complex

	MZ-Ga	MZ-Lga		LZ-Ga and UZ-Ga					UZ-Qga		IZ		
		core	rim	core	cor-rim	rim	core	rim	core	core			
SiO_2	45.22[a]	45.80	54.64[a]	46.03	55.47	57.50	47.58	55.63	56.67	46.17	50.37	57.36	62.17
Al_2O_3	35.33	34.79	28.33	34.85	28.32	26.28	33.32	27.92	28.18	35.14	31.45	26.77	23.50
FeO	0.26	0.15	0.09	0.17	0.15	0.13	0.25	0.10	0.14	0.24	0.15	0.15	0.12
CaO	18.06	17.12	10.69	18.06	10.58	8.19	16.32	10.03	9.52	17.61	14.41	8.84	4.90
Na_2O	1.08	1.38	5.46	1.22	5.39	6.88	2.13	5.72	6.09	1.53	3.28	6.45	8.54
K_2O	0.0	0.03	0.14	0.0	0.10	0.11	0.04	0.05	0.23	0.03	0.04	0.26	0.36
tot	99.95	99.27	99.35	100.33	100.01	99.09	99.64	99.45	100.83	100.72	99.70	99.83	99.59

Analysis marked with [a] have been used in the major element modelling (see text)

Table 2. Selected pyroxene analyses, Punta Falcone gabbroic complex

	MZ-Ga	MZ-Lga	LZ-Ga	UZ-Ga	UZ-Qga
SiO_2	52.98[a]	52.74[a]	52.44	52.70	52.71
TiO_2	0.23	0.22	0.12	0.17	0.12
Al_2O_3	1.59	1.23	0.95	0.83	0.65
Cr_2O_3	0.0	0.0	0.0	0.0	0.04
FeO	17.23	9.45	9.39	8.67	9.82
MnO	0.45	0.37	0.40	0.33	0.55
MgO	25.29	14.03	13.35	14.52	12.94
CaO	1.23	21.81	23.02	22.08	22.71
Na_2O	0.0	0.20	0.22	0.16	0.22
Tot	99.00	100.03	99.89	99.46	99.75

Analysis marked with [a] have been used in the major element modelling (see text)

zoning textures are ubiquitous in all gabbroic units, in particular they are more abundant in the UZ-Qga (Table 1).

Orthopyroxene occurs as a cumulus phase in theMZ-Ga, and it is enclosed in the tschermakite oikocrysts. Its composition ($\sim En_{70}$) points to crystallization from an already fractionated mafic magma, as it is also indicated by the absence of olivine in the Punta Falcone gabbroic complex (e.g. Perfit et al. 1980).

Clinopyroxene ($\sim Wo_{44}En_{40}Fs_{16}$) occurs as irregular and resorbed crystal in amphibole cores. Its low Al_2O_3 content (0.65-1.20 wt%, Table 2) is suggestive of crystallization at low pressures (Green and Ringwood 1968).

Calcic amphiboles show a wide variety of habits and compositions in the different gabbroic units. They are brown to pale-green crystals, and usually are interstitial between plagioclase, forming homoaxial rims around clinopyroxene, but they also occur as subhedral to euhedral crystals, in particular in the LZ-Ga, UZ-Ga, and IZ rocks. No consistent optical or chemical zonation of single amphibole grains is apparent within each gabbroic unit, except for amphiboles immediately adjacent to biotite crystals and for amphiboles rimming clinopyroxene.

The type of amphibole progressively varies in composition from pargasite to Mg-hornblende, passing from the large oikocrysts of the MZ-Ga to the anhedral crystals of the UZ-Qga (Fig. 3A). This fact suggests that the tschermakite-type substitution ($Al^{IV} + Al^{VI} \leftrightarrow Mg + Si$) has been operative during crystallization of these amphiboles. Amphiboles forming rims around clinopyroxene, display a different, well defined trend towards actinolite compositon (Fig. 3A), pointing to an origin by replacement of clinopyroxene (e.g. Nakajima and Ribbe 1981).

In the IZ, amphiboles define a different trend from those of the gabbroic units. They are Mg-hornblendes and ferro-edenitic hornblendes (Table 3), and show a decrease of Si content in tetrahedral site joined by an increase of A-site occupancy with decreasing Mg# [$100\,Mg/(Mg + Fe^{2+})$] (Fig. 3B), suggesting the occurrence of edenite-type substitution ($Na + Al^{IV} \leftrightarrow Si$).

Biotite is a ubiquitous mafic phase in the gabbroic complex, even though it is not present in large amounts. It occurs as brownish subhedral crystals, and shows a decrease in Mg# from 64 to 57 (LZ, MZ, UZ), and from 59 to 40 (IZ). In the MZ-Ga, some phlogopites (Mg# 77-88) are found as aggregates with magnetite crystals and display replacement features on pargasite.

Among the other phases, fibrous amphiboles belonging to the cummingtonite-grunerite series occur in the MZ units (Table 3), and may have been formed by replacement of orthopyroxene (e.g. Nakajima and Ribbe 1981). Magnetite and ilmenite (Table 4) occur in larger amount in the UZ-Ga and LZ-Ga than in other units. Quartz occurs as anhedral crystals in all rocks of the gabbroic complex. The presence of K-feldspar is restricted to the UZ-Qga and IZ rocks, and it is always strongly perthitic and poikilitic. Accessory phases consist of apatite and zircon, even though the latter is only present in the UZ-Qga and IZ rocks.

Application of the amphibole-plagioclase geothermometer (Blundy and Holland 1990) yields crystallization temperatures of about 980–1010°C and 770–820°C, for amphibole-plagioclase pairs of the gabbroic units and IZ rocks, respectively.

In addition, the presence of the required mineral assemblage in the most evolved IZ rocks, permits the application of the hornblende geobarometer by Hammarstrom and Zen (1986), which yields pressures of crystallization of about 3–4 kbar. This range of crystallization pressure can reasonably be extrapolated to the whole gabbroic complex, as it is also indicated by the low Al_2O_3 content of clinopyroxene. The same pressure has been estimated for the crystallization of the surrounding granite stock (Poli and Tommasini 1991a).

Geochemistry

Representative samples of the Punta Falcone gabbroic complex have been analyzed for both major and trace elements (Table 5). Major elements have been determined by X-ray fluorescence spectrometry, with full matrix correction after Franzini and Leoni (1972), except MgO and Na_2O which were determined by atomic absorption spectrometry and FeO by titration. V, Cr, Co, Ni, Rb, Sr, Y, Zr, Nb, and Ba were determined by XRF after Kaye (1965) and Sc, Hf, Ta, Th, and REE by instrumental neutron activation analysis after Poli et al. (1977). The precision is better than 15% for Ba, Nb, V, Lu, and Tb, better than 10% for Cr, Y, Zr, Ta, and Yb, and better than 5% for all the other elements. The accuracy has been tested on international standards and is better than 10%.

Five types of behaviours can be defined on Harker diagrams using MgO as the differentiation index (Fig. 4):

(1) TiO_2 is positively correlated with MgO for the LZ, UZ, and IZ rocks; whereas the MZ-Ga and MZ-Lga rocks display lower TiO_2 content than other rocks of the

Table 3. Selected amphibole analyses, Punta Falcone gabbroic complex

	Magmatic amphiboles[a]								Reaction amphiboles[b]					
	MZ-Ga FPaHb	MZ-Lga TscHb	LZ-MgHb	UZ-Ga FPaHb	UZ-Qga MgHb	IZ MgHb	MgHb	FEdHb	MZ-Ga MgHb	MZ-Lga Act	LZ-AcHb	UZ-Ga AcHb	MZ-Ga Cum	MZ-Lga Cum
SiO_2	42.67	43.10	47.29	42.78[c]	46.08	45.44	44.68	42.62	48.48	53.01	50.88	50.90	54.21	53.54
TiO_2	3.20	2.51	1.10	2.93	1.08	1.39	1.33	1.89	0.91	0.11	0.58	0.98	0.05	0.07
Al_2O_3	12.10	11.75	6.84	10.43	7.70	7.52	8.21	9.41	6.88	3.57	4.65	3.98	0.52	1.28
Cr_2O_3	0.06	0.0	0.0	0.0	0.0	0.0	0.03	0.0	0.0	0.02	0.02	0.0	0.0	0.01
FeO	13.59	13.54	15.91	14.07	17.16	17.31	18.20	20.60	12.90	10.18	13.71	11.20	18.85	17.83
MnO	0.19	0.29	0.29	0.21	0.37	0.49	0.45	0.54	0.20	0.29	0.28	0.26	0.53	0.70
MgO	12.88	12.91	12.78	12.53	11.85	11.61	10.36	8.18	16.01	17.91	14.82	16.32	20.41	19.61
CaO	11.32	11.47	11.94	11.70	11.99	11.65	11.76	11.17	10.97	11.89	12.19	12.03	1.24	3.48
Na_2O	1.61	1.20	0.71	1.47	0.80	0.84	1.00	1.10	0.83	0.33	0.42	0.45	0.0	0.02
K_2O	0.50	0.51	0.44	0.62	0.76	0.71	0.88	0.14	0.43	0.04	0.20	0.16	0.0	0.0
Tot	98.12	97.28	97.30	96.74	97.79	96.96	96.90	96.65	97.61	97.35	97.75	96.28	95.81	96.54

[a]amphiboles crystallized directly from the magma; [b]amphiboles formed by reaction between magma and pyroxenes. Analysis marked with [c] has been used in the major element modelling. FPaHb: ferroan pargasitic hornblende; TscHb: tschermakitic hornblende; MgHb: magnesio hornblende; FEdHb: ferroan edenitic hornblende; Act: actinolite; AcHb: actinolitic hornblende; Cum: cummingtonite

Table 4. Selected oxide analyses, Punta Falcone gabbroic complex

	Magnetite		Ilmenite	
	MZ-Lga	UZ-Qga	MZ-Ga	MZ-Lga
TiO_2	0.18[a]	0.27	48.00	49.28[a]
Al_2O_3	0.41	0.0	0.0	0.0
Fe_2O_3	68.74	68.40	8.40	7.45
Cr_2O_3	0.04	0.0	0.04	0.0
FeO	31.53	31.18	41.21	41.26
MnO	0.03	0.08	1.83	2.70
MgO	0.0	0.0	0.0	0.0
CaO	0.0	0.0	0.08	0.25
Tot	100.93	99.93	99.56	100.94

Fe_2O_3 determined by stoichiometry.
Analyses marked with [a] have been used in the major element modelling (see text)

same MgO content. This behaviour is also followed by FeO_{tot}, Sc, Co, and V.

(2) Sr shows a bell-shaped trend against MgO for the LZ, UZ, and IZ rocks. The MZ units, in particular the MZ-Lga, have higher Sr content than other rocks of the same MgO content. This behaviour is also followed by Al_2O_3, and CaO.

(3) Cr is positively correlated with MgO for all rocks of the gabbroic complex. This behaviour is also followed by Ni.

(4) Y displays smooth variations against MgO for the LZ, MZ, and UZ units whereas the IZ rocks fit a fairly negative correlation. This behaviour is also followed by SiO_2, Na_2O, Rb, Th, Ta, Hf, Zr, Nb, and REE (except Eu). It is noteworthy that by comparison with the host granite, the trend defined by the IZ rocks plots towards higher concentrations of all these components (except SiO_2 and Rb).

(5) Ba has the same behaviour as Y, except for the most evolved IZ sample (SP32). This sample, whose Ba content drops below that of the host-granite, plots out of the trend defined by other IZ rocks. This behaviour is also followed by K_2O, P_2O_5, and Eu.

It is noteworthy that the representative sample of the dike-like bodies outcropping at the northwestern edge of the gabbroic complex (Fig. 1) follows the same elemental behaviour as the IZ rocks (Fig. 4), supporting field observations which indicate they are detached, dike-like fragments from the IZ.

The chondrite-normalized REE patterns for the Punta Falcone gabbroic units are reported in Fig. 5A. The LZ, MZ, and UZ units display variable LREE fractionation (La/Sm = 2.9-4.4), and smooth HREE fractionation (Tb_n/Yb_n = 0.96–1.36). All samples also have negligible Eu anomalies (Eu/Eu* = 0.93-1.19). The enrichment factor for La progressively varies from 22 to 45 × chondrite, passing from the LZ-Ga to the UZ-Qga (Fig. 5A).

The REE patterns of the IZ rocks exhibit an increase in both the negative Eu anomaly (Fig. 5B), and HREE fractionation (Table 5) with evolution. Moreover, enrichment factors for LREE display a wider range than that of the gabbroic units, in particular La varies from 42 to 174 × chondrite, from the least to the most evolved IZ sample, respectively (Fig. 5B).

Estimation of the parental magma composition

A common problem in studying mafic layered intrusions is the estimation of the parental magma composition, inasmuch as the bulk chemical composition of rock samples is unlikely to match that of the parental magma because of the occurrence of cumulus processes (e.g. Irvine 1979).

The chilled margin method to obtain the parental magma composition (e.g. Wager and Brown 1967) cannot be applied to the Punta Falcone gabbroic complex, because extensive interaction processes have been operative along contacts with the surrounding granite stock, and have modified the composition of the "frozen" mafic magma (IZ). The parental magma composition can also be estimated by the weighted summation method (e.g. Ragland and Butler 1972; Klewin 1990). This method has been applied to the Punta Falcone gabbroic complex,

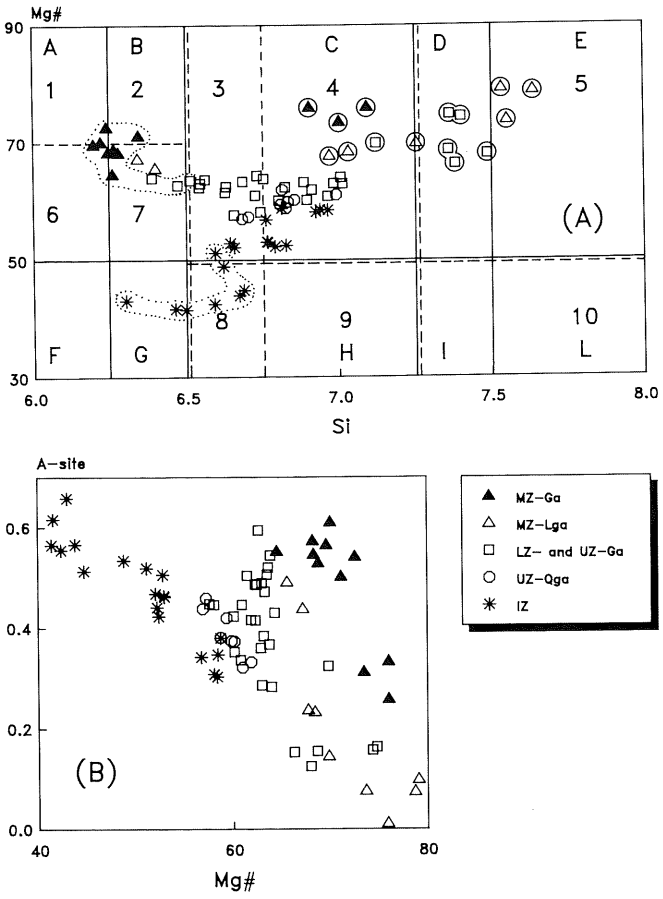

Fig. 3. A Classification diagram for calcic amphiboles (Leake 1978). *Solid lines* define classification fields for amphibole with A-site occupancy < 0.5. A, Tschermakite; B, Tschermakitic hornblende; C, Mg-hornblende; D, Actinolitic hornblende; E, Actinolite; F, Ferro-tschermakite; G, Ferro-tschermakitic hornblende; H, Ferro-hornblende; I, Ferro-actinolitic hornblende; L, Ferro-actinolite. *Dashed lines* define classification fields for amphiboles with A-site occupancy > 0.5. 1 = Pargasite; 2 = Pargasitic hornblende; 3 = Edenitic hornblende; 4 = Edenite; 5 = Silicic edenite; 6 = Ferroan pagasite; 7 = Ferroan pargasitic hornblende; 8 = Ferro-edenitic hornblende; 9 = Ferro-edenite; 10 = Silicic-ferro edenite. *Dotted fields*, amphiboles with A-site > 0.5; all other amphiboles have A-site < 0.5. *Circled symbols*, amphiboles formed by reaction between the liquid and clinopyroxene. **B** Diagram of A-site occupancy versus Mg # $[100\ Mg/(Mg + Fe^{2+})]$ for calcic amphiboles

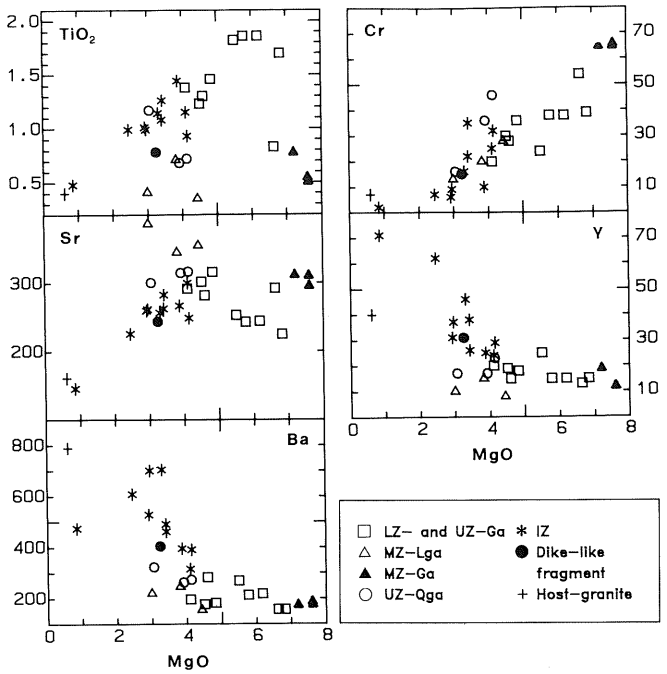

Fig. 4. Harker diagrams illustrating the main trends exhibited by rock samples of the Punta Falcone gabbroic complex

summing the average chemical compositon of each unit, weighted according to its outcrop surface. However, the limit of this crude estimation is twofold: i) it does not take into account the third dimension, i.e. the volume of each gabbroic unit; ii) it assumes that crystallization occurred without loss or gain of material. The first point is, of course, unsolvable, except perhaps by considering volume estimations from geological sections. This would yield, however, as much uncertainty as the outcrop surface method, owing to the high subjectivity of drawing geological sections in intrusive rocks. With respect to the second point, field observations indicate that the mafic magma was emplaced in a single, relatively rapid injection and crystallized without loss of material. However, gain of material from the surrounding granite stock cannot be ruled out, in particular for the IZ rocks. In fact, the high compositional variability of the IZ rocks (Table 5) in such a narrow outcrop surface (Fig. 1), suggests the occurrence of extensive interaction processes with the host-rock, which drastically changed their major and trace element compositions. Accordingly, the IZ rocks have been excluded from the computation.

Bearing these reservations in mind, the calculated major element composition of the parental magma is reported in Table 6. This composition is very close to three samples of the UZ-Ga (SP79, SP98, SP97, Table 5). This chemical feature along with the fact that these samples have no textural evidence for the occurrence of crystal accumulation, suggests that they could be considered representative of the parental mafic magma. Their major and trace element contents, for instance SiO_2, TiO_2, Al_2O_3, MgO abundances (Table 5), REE patterns (Fig. 5a), and LILE/HFSE ratios (e.g. Th/Ta = 10) clearly indicate a calc-alkaline affinity (Sun 1980; Pearce 1982), in agreement with the general tectonomagmatic setting in Sardinia during the Carboniferous (Poli et al. 1989). These samples are compositionally similar to evolved high alumina basalts (Perfit et al. 1980).

In contrast, all the other samples have textural and/or chemical features indicating they are cumulate rocks. The MZ-Ga and MZ-Lga have both textural (orthocumulate textures) and chemical (Fig. 4) features indicating they were affected by crystal accumulation of plagioclase and pyroxenes. In fact, the MZ-Ga and MZ-Lga are displaced with respect to the samples considered representative of the parental magma (UZ-Ga′, Fig. 6) just towards plagioclase-orthopyroxene, and plagioclase-clinopyroxene tie-lines, respectively.

The LZ-Ga, UZ-Ga, and UZ-Qga have no textural evidence of crystal accumulation; however, conflicting

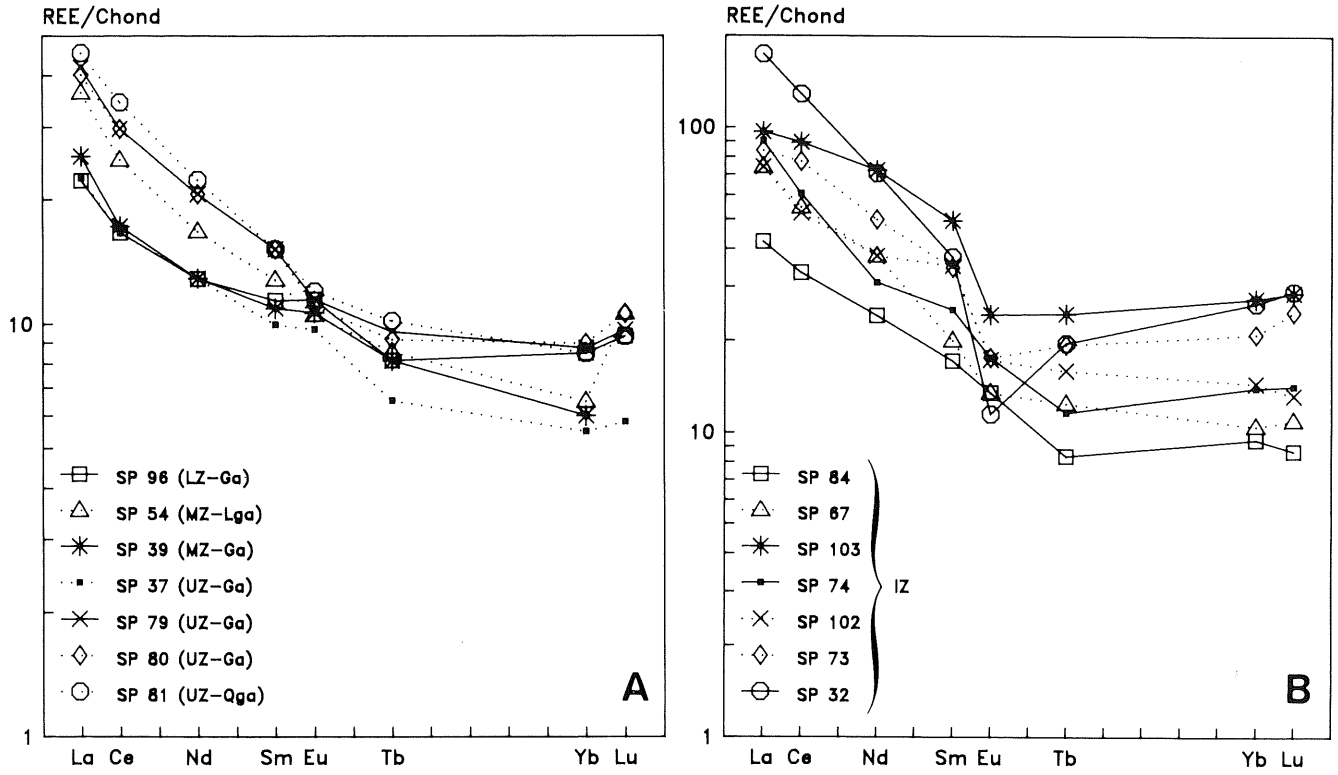

Fig. 5. Chondrite-normalized (Haskin et al. 1966) REE patterns of the gabbroic units (**A**), and IZ rocks (**B**)

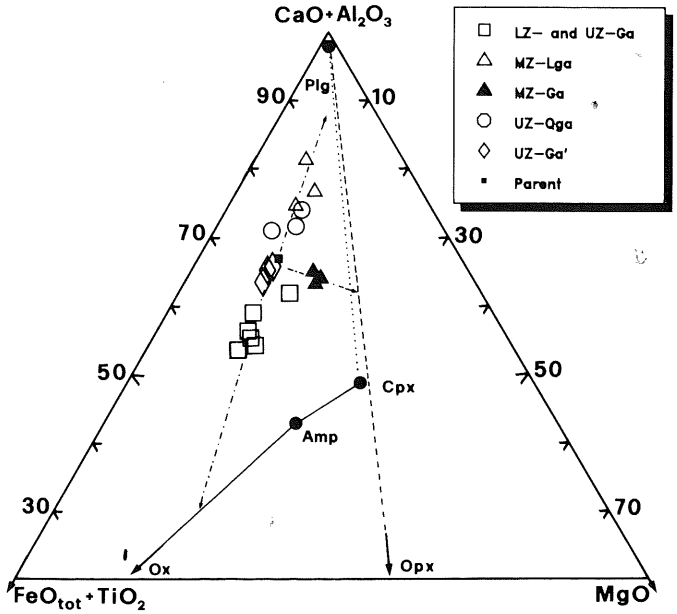

Fig. 6. Triangular diagram illustrating the effects of cumulus processes on the different gabbroic units. A different symbol (*open diamond*) has been used for samples (UZ-Ga′) resembling the estimated parental magma composition. *Dashed-dotted vectors* indicate the displacement of the cumulate units towards tie-lines of cumulus minerals. *Solid line*, clinopyroxene-amphibole-oxides tie-line; *dashed line*, plagioclase-orthopyroxene tie-line; *dotted line*, plagioclase-clinopyroxene tie-line

evidence arises in considering the LZ-Ga and UZ-Ga (excluding UZ-Ga′) as liquids: their low SiO_2 (45%) and slightly high TiO_2 (1.7%) contents indicate an alkaline affinity and contrast with the REE patterns (Fig. 5a) and LILE/HFSE ratios which point to a calc-alkaline affinity (Pearce and Cann 1973; Wood et al. 1979). In addition, geochemical data suggest the occurrence of cumulus processes even in these units (Fig. 6). In fact, the LZ-Ga and UZ-Ga (excluding UZ-Ga′) are displaced with respect to the UZ-Ga′ samples towards clinopyroxene-amphibole-oxides tie-lines, whereas the UZ-Qga are displaced towards the plagioclase-clinopyroxene tie-line.

Differentiation of the gabbroic units

A model of low-pressure, closed-system in-situ crystallization is proposed for the differentiation of the Punta Falcone gabbroic units. The mafic magma was emplaced in a single, relatively rapid injection, and crystallization commenced throughout. The "frozen" IZ rocks, formed along contacts with the surrounding granite stock, further retarded the cooling rate permitting more extensive growth of crystal nuclei.

The following order of crystallization is proposed for the gabbroic units on the basis of petrographic and mineral chemistry data. Plagioclase (An_{90-87}) + orthopyroxene + clinopyroxene nucleated at the very beginning of crystallization for a very short period as indicated

by the small modal abundance of pyroxenes (Fig. 2). Plagioclase, grading from An_{90} to An_{40}, + calcic amphiboles + oxides followed in the crystallization sequence and were successively joined by the crystallization of biotite + quartz ± K-feldspar. The first nucleating minerals represent cumulus phases. In contrast, the other minerals grade from intercumulus phases in the first cumulate rocks (e.g. pargasite in the MZ-Ga), to cumulus phases in the later crystallizing rocks (e.g. ferroan pargasitic hornblende in the LZ-Ga).

The hydrous phases crystallized in response to an increase in volatile activity due to the early crystallization of anhydrous phases, as it has been documented in experimental studies (e.g. Baker and Eggler 1983). On the basis of microstructural evidence pargasite, tschermakite, Mg-hornblende, and biotite crystallized directly from the evolving liquid, whereas actinolite, cummingtonite, and phlogopite formed by reaction between the liquid and clinopyroxene, orthopyroxene, and tschermakite, respectively. The crystallization sequence in the gabbroic units, the high An content of plagioclase (An_{90-85}), and the occurrence of orthopyroxene, not recorded in high-alumina basalts crystallizing under dry conditions (Green and Ringwood 1968), suggest crystallization under wet conditions. Moreover, the estimation of the crystallization temperature on amphibole-plagioclase pairs in the gabbroic units (~1000°C), indicates a water content in the magma of ~4–5 wt%, and a liquidus temperature of about 1100–1150°C (Baker and Eggler 1983, Fig. 3). The water content in the magma is close to the water-saturated curve for basalts at 3-4 kbar (Holloway and Burnham 1972; Hughes 1982).

Table 5. Major (wt%) and trace element (ppm) analyses of the Punta Falcone gabbroic complex

	Lower Zone			Middle Zone						Upper Zone					
	LZ-Ga			MZ-Ga			MZ-Lga			UZ-Ga					
Class.	SP 96 GA	SP 69 GA	SP 82 GA	SP 72 GA	SP 71 GA	SP 39 GA	SP 70 LGA	SP 77 LGA	SP 54 LGA	SP 75 GA	SP 37 GA	SP 80 GA	SP 79 GA	SP 98 GA	SP 97 GA
SiO_2	44.39	47.02	47.95	49.41	49.83	50.31	49.92	50.22	50.70	45.50	45.62	49.36	49.69	50.50	50.76
TiO_2	1.70	1.82	0.83	0.78	0.51	0.55	0.35	0.41	0.71	1.86	1.86	1.46	1.30	1.38	1.23
Al_2O_3	16.56	15.39	19.12	20.38	20.02	19.57	23.60	24.89	22.29	16.66	16.98	16.71	18.75	18.80	18.99
Fe_2O_3	5.47	6.57	3.61	2.32	1.90	1.77	2.24	1.70	2.67	6.14	5.55	5.71	3.94	4.01	3.38
FeO	9.76	8.59	7.26	6.12	6.72	6.91	3.67	3.60	4.48	8.72	9.14	6.75	6.91	5.81	6.35
MnO	0.20	0.19	0.16	0.14	0.15	0.16	0.10	0.09	0.12	0.16	0.17	0.15	0.14	0.13	0.14
MgO	6.83	5.50	6.63	7.20	7.61	7.60	4.43	2.99	3.81	6.18	5.77	4.83	4.60	4.10	4.51
CaO	10.99	9.83	10.17	10.27	9.68	9.61	10.84	11.99	11.20	10.94	11.09	9.53	10.57	9.13	10.40
Na_2O	1.28	1.60	1.46	1.46	1.28	1.36	1.75	1.64	1.57	1.24	1.15	1.86	1.65	2.05	1.57
K_2O	0.54	0.99	0.42	0.49	0.54	0.54	0.79	0.73	0.84	0.63	0.58	0.80	0.95	1.25	1.16
P_2O_5	0.08	0.10	0.08	0.05	0.05	0.07	0.07	0.12	0.13	0.05	0.07	0.13	0.12	0.08	0.10
LOI	2.21	2.40	2.30	1.38	1.70	1.56	2.23	1.62	1.47	1.92	2.03	2.72	1.38	2.76	1.39
Mg#	49.4	44.3	57.0	64.8	65.4	65.0	62.0	55.0	53.7	47.6	46.1	46.0	47.9	47.7	50.2
Sc	50					28			21		47	35	30		
V	780	582	344	194	168	145	111	106	199	836	834	556	483	437	325
Cr	39	24	54	65	66	65	28	13	20	38	38	36	28	20	30
Co	62	50	43	37	36	36	20	20	25	65	56	42	33	35	31
Ni	10	8	12	23	21	22	10	11	8	10	9	15	8	10	7
Rb	25	35	13	9	10	10	42	25	33	17	14	25	25	47	43
Sr	225	253	292	312	296	311	355	387	345	244	243	316	282	292	302
Y	15	25	13	19	12	12	8	10	15	15	15	18	15	20	19
Zr	63	78	62	64	53	71	41	80	79	61	58	96	78	85	60
Nb	7	7	10	7	5	11	5	8	10	11	8	12	8	7	5
Ba	157	269	157	176	177	189	155	220	246	218	213	182	283	196	177
Hf	1.8					1.3			1.6		1.6	2.0	1.9		
Ta	0.20					0.20			0.29		0.15	0.25	0.27		
Th	1.3					1.1			1.9		1.6	3.2	2.7		
La	6.9					7.6			11.3		7.0	12.5	13.0		
Ce	14.0					14.5			21		14.0	25	25		
Nd	7.5					7.5			9.8		nd	12	12		
Sm	2.4					2.3			2.7		2.1	3.2	3.2		
Eu	0.85					0.79			0.78		0.72	0.82	0.85		
Tb	0.40					0.40			0.42		0.32	0.45	0.47		
Yb	1.7					1.2			1.3		1.1	1.8	1.8		
Lu	0.29					nd			0.33		0.18	0.33	0.30		
Tb_n/Yb_n	0.96					1.36			1.32		1.19	1.02	1.10		
Eu/Eu*	1.19					1.09			0.98		1.18	0.93	0.94		
REE	43					43			57		33	67	68		

Composition of the host-granite from Poli and Tommasini (1991a); SP 95 is the representative sample of the dike-like fragments of IZ outcropping at the northwestern edge of the Punta Falcone gabbroic complex. nd = not determined; Mg# = 100 Mg/(Mg + Fe^{2+}) mol%; classification: GA = gabbro; LGA = leucogabbro; QGA-quartz-gabbros; QD = quartz-diorite; T = tonalite; GD = granodiorite; MGR = monzogranite

Table 5 (continued)

	Upper zone			Interaction Zone										Dike	Host-gr
	UZ-QGa														
Class.	SP 62 QGA	SP 76 QGA	SP 81 QGA	SP 84 QGA	SP 67 QD	SP 147 T	SP 103 T	SP 93 T	SP 74 T	SP 102 T	SP 73 GD	SP 104 T	SP 32 GD	SP 95 T	SP 58 MGR
SiO_2	52.53	53.28	53.34	52.60	53.56	56.22	56.36	57.24	57.30	58.86	59.28	59.59	68.12	57.88	71.34
TiO_2	0.72	0.68	1.17	1.15	1.44	1.26	1.14	0.93	1.08	0.99	0.99	1.01	0.48	0.78	0.40
Al_2O_3	20.28	20.83	20.30	17.00	16.74	16.21	16.97	16.85	16.71	16.67	16.80	16.48	15.49	17.80	14.55
Fe_2O_3	2.47	2.52	3.18	4.36	3.66	3.88	2.73	2.42	3.17	2.48	2.33	2.49	0.51	2.62	1.14
FeO	4.70	3.91	5.03	5.60	7.10	5.40	5.72	5.12	5.18	5.15	4.91	4.91	3.47	4.41	1.70
MnO	0.13	0.11	0.10	0.15	0.18	0.16	0.13	0.15	0.14	0.13	0.14	0.12	0.10	0.12	0.06
MgO	4.13	3.91	3.05	4.10	3.87	3.42	3.30	4.14	3.41	2.95	2.45	2.92	0.85	3.24	0.61
CaO	9.53	9.90	9.40	10.09	8.45	7.07	6.14	6.39	6.65	6.19	5.63	5.68	2.74	5.98	2.11
Na_2O	2.29	2.00	1.87	1.71	2.00	2.83	2.94	2.79	2.65	2.90	3.11	3.00	3.88	3.44	3.11
K_2O	0.95	1.00	1.31	1.20	1.18	2.64	2.73	2.17	2.25	2.10	2.99	2.11	3.03	1.41	4.14
P_2O_5	0.07	0.09	0.05	0.22	0.21	0.17	0.22	0.09	0.14	0.17	0.20	0.19	0.19	0.13	0.11
LOI	2.21	1.77	1.20	1.82	1.62	0.74	1.61	1.72	1.31	1.41	1.17	1.50	1.13	2.18	0.73
Mg #	55.5	57.0	44.7	47.4	43.8	44.6	45.8	54.3	47.1	45.6	42.3	46.1	31.2	50.1	31.9
Sc			22	30	33		26		26	20	23		10.70		7.5
V	156	146	402	337	268	210	186	163	208	166	169	159	41	166	41
Cr	46	36	16	25	10	35	16	32	22	9	7	6	2	15	7
Co	23	19	27	31	31	23	19	21	25	18	17	18	6	20	5
Ni	10	9	8	13	5	10	8	14	8	5	5	4	5	5	3
Rb	30	27	43	38	43	81	96	88	68	85	109	96	140	77	163
Sr	317	315	301	300	267	283	257	249	263	262	226	260	146	244	161
Y	23	17	17	24	25	26	46	29	38	37	62	31	71	31	40
Zr	89	101	107	78	58	117	207	137	149	189	159	186	241	176	197
Nb	6	7	8	10	13	13	23	12	15	15	19	15	22	12	17
Ba	273	263	323	315	395	461	704	390	490	700	608	527	474	404	789
Hf			2.7	1.7	1.7		5.7		3.2	3.9	4.0		7.5		4.7
Ta			0.35	0.31	0.55		1.0		0.85	0.55	1.2		1.5		1.1
Th			4.7	3.0	6.1		8.9		6.0	3.6	8.0		21		14.7
La			14.1	13.1	23		30		nd	23	26		54		39
Ce			29	28	46		75		51	44	65		108		81
Nd			13	14	22		42		18	22	29		41		29
Sm			3.2	3.6	4.2		10.4		5.3	7.4	7.3		7.9		5.4
Eu			0.89	1.00	1.00		1.80		1.30	1.28	1.30		0.85		0.95
Tb			0.50	0.41	0.61		1.20		0.57	0.78	0.95		0.96		0.65
Yb			1.7	1.9	2.1		5.5		2.8	2.9	4.2		5.3		2.1
Lu			0.29	0.27	0.34		0.89		0.44	0.41	0.77		0.90		0.30
Tb_n/Yb_n			1.20	0.88	1.19		0.89		0.83	1.10	0.92		0.74		1.26
Eu/Eu*			0.95	1.14	0.84		0.71		1.04	0.72	0.68		0.44		0.68
REE			75	73	115		198		124	121	160		249		178

Composition of the host-granite from Poli and Tommasini (1991a); SP 95 is the representative sample of the dike-like fragments of IZ outcropping at the northwestern edge of the Punta Falcone gabbroic complex. nd = not determined; Mg# = 100 Mg/(Mg + Fe^{2+}) mol%; classification: GA = gabbro; LGA = leucogabbro; QGA-quartz-gabbros; QD = quartz-diorite; T = tonalite; GD = granodiorite; MGR = monzogranite

Major element modelling

The different units of the Punta Falcone gabbroic complex can be accounted for by mixtures between cumulus phases and trapped (evolved) liquids formed during the crystallization of the parental magma. In order to evaluate such a process, a mathematical artifice has been developed because the chemical compositon of trapped liquids cannot be directly determined, and to avoid uncertain estimations of cumulus-intercumulus proportions by thin section modal analyses.

In general, considering a closed system and subdividing the crystallization into n steps, after each step i the respective liquid (L_i) can be subdivided into a solid and an evolved liquid phase. The composition of each liquid (L_i) is given on the basis of mass-balance criteria by:

$$L_i = y_i S_i + (1 - y_i) EL_i \quad (1)$$

where S_i and EL_i represent the bulk chemical composition of the solid and evolved liquid phase, respectively, and y_i represents the mass fraction of crystallized minerals forming the solid phase after each step i. It is noteworthy that for $i = 1$, L_1 represents the composition of the parental magma, whereas for $i > 1$, L_i represents the composition of the evolved liquid from step $i - 1$ (EL_{i-1}). Moreover, a gabbroic unit formed at step i, can be subdivided into a cumulus and an intercumulus assemblage, and its composition (GU_i) is given by:

$$GU_i = rCA_i + (1 - r) IA_i \quad (2)$$

Table 6. Estimated parental magma composition according to the weighted summation method

	LA-Ga	MZ-Ga	MZ-Lga	UZ-Ga	UZ-Ga	UZ-Qga	PARENT
n	2	3	3	4	2	3	
#	27.5%	2.1%	32.0%	8.8%	2.8%	26.8%	
	(a)	(a)	(a)	(a)	(a)	(a)	
SiO_2	45.71	49.85	50.28	49.14	47.43	53.05	49.58
TiO_2	1.76	0.61	0.49	1.47	1.66	0.86	1.06
Al_2O_3	15.98	19.99	23.59	18.38	16.69	20.47	19.93
Fe_2O_3	6.02	2.00	2.20	4.22	5.93	2.72	3.67
FeO	9.18	6.58	3.92	7.05	7.74	4.55	5.97
MnO	0.19	0.15	0.10	0.14	0.15	0.11	0.13
MgO	6.17	7.47	3.74	4.74	5.51	3.70	4.62
CaO	10.41	9.85	11.34	10.30	10.24	9.61	10.47
Na_2O	1.44	1.37	1.65	1.61	1.55	2.05	1.69
K_2O	0.77	0.52	0.79	0.98	0.71	1.09	0.87
P_2O_5	0.09	0.06	0.11	0.08	0.09	0.07	0.09
LOI	2.30	1.55	1.77	1.89	2.32	1.73	1.91

n: number of averaged samples
#: percentage of the outcrop surface of each unit
(a): averaged composition
The two lenses of UZ-Ga (Fig. 1) have been separately averaged

where CA_i and IA_i represent the bulk chemical composition of the cumulus and intercumulus assemblage, respectively, and r represents the mass fraction of cumulus minerals in the gabbroic unit. The intercumulus assemblage (IA_i) consists of those minerals crystallized from the evolved liquid phase (EL_i) after the occurrence of *i*-th step of crystallization. Therefore, with respect to bulk chemical composition $IA_i = EL_i$.

Then, solving Eq. 1 with respect to EL_i and substituting into Eq. 2, yields:

$$GU_i = rCA_i - h_i y_i S_i + h_i L_i \quad (3)$$

where $h_i = (r - y_i)/(1 - y_i)$. Moreover, the chemical composition of the solid phase (S_i) and of the cumulus assemblage (CA_i) can be written as linear combinations:

$$S_i = \sum a_{ik} M_{ik} \qquad \text{for } k = 1 \text{ to } np_i \quad (4)$$

$$CA_i = \sum b_{ik} M_{ik} \qquad \text{for } k = 1 \text{ to } np_i \quad (5)$$

where np_i and M_{ik} are the number of mineral phases crystallized at step *i* and their chemical composition, respectively; a_{ik} and b_{ik} are the mass fraction of the *k*-th mineral phase in the solid phase and in the cumulus assemblage, respectively.

Substituting Eqs. 4 and 5, Eq. 2 can be rearranged to give:

$$GU_i = \sum z_{ik} M_{ik} + h_i L_i \quad (6)$$

where $z_{ik} = (rb_{ik} - h_i y_i a_{ik})$.

Accordingly, the formation of different gabbroic units related to the *i*-th step of crystallization, can be modelled by simple mixtures between the *i*-th liquid (L_i) and different percentages of minerals formed after the *i*-th step of crystallization. It is noteworthy that the amounts of minerals added to the *i*-th liquid (Eq. 6) do not match the actual amounts of cumulus minerals in the *i*-th gabbroic unit (r, Eq. 2). They simply represent the mass fractions of minerals that must be added to the *i*-th liquid to account for the composition of the *i*-th gabbroic unit. From a qualitative standpoint this fact is also evident from Fig. 6.

The proposed mathematical model has been applied to the Punta Falcone gabbroic units subdividing the crystallization into two steps. The first step concerns the anhydrous crystallization of plagioclase and pyroxenes, taking place for a short period and generating the MZ-Ga unit. The second step concerns the hydrous crystallization of plagioclase + calcic amphiboles + oxides, taking place for a longer period and generating the other gabbroic units.

Then, a quantitative estimation has been performed to achieve both z_{ik} and h_i mass fraction in each unit (Eq. 6), using a major element mixing computation, and taking into account both petrographic data and crystallization sequence. The composition of the liquid phase (L_i) has been assumed equal to that of the estimated parental magma (Table 6) for both steps of crystallization. This assumption is not corrent for step 2, because the composition of L_2 is equal to that of the evolved liquid from step 1 ($L_2 = EL_1$). However, conservative estimations yield a compositonal difference between L_1 and L_2 less than 1%. In fact, step 1 concerns the formation of the MZ-Ga unit, which has an outcrop surface of 2.1% (Table 6). This unit consists of orthocumulate rocks, which have at most 70% of cumulus crystals (plagioclase and orthopyroxene). Thus, the amount of solid phase developed during step 1 (y_1, equation 1) is roughly 1.5% of the total system, and therefore the compositional difference between L_1 and L_2 is negligible and does not affect the following computations.

The results of the mixing process are reported in Table 7. They show reasonable values of squares of residuals excluding UZ-Qga, and indicate that: (1) the MZ-Ga could be a mixture between the parental magma (~58%) and fairly equal amounts (~20%) of plagioclase and orthopyroxene; (2) the LZ-Ga and UZ-Ga, excluding those samples whose composition is equivalent to the parental

Table 7. Major element modelling of the Punta Falcone gabbroic complex. The percentages of the different minerals added to the parental magma to achieve the composition of representative samples of the different units are reported. Estimations on water-free basis

	Step I MZ-Ga		Step II LZ-Ga	MZ-Lga		UZ-Ga		UZ-Qga	
	SP 71	SP 39	SP 96	SP 77	SP 54	SP 37	SP 75	SP 81	SP 76
Parental magma	56.9	59.9	52.6	56.6	74.5	69.0	66.4	95.6	87.2
Plg (An_{90})	22.9	20.6	7.5	22.3	9.4	5.2	3.9	4.4	12.8
Plg (An_{52})	–	–	–	20.2	14.5	–	–	–	–
Clinopx	–	–	1.5	0.9	1.6	7.2	5.2	–	–
Orthopx	20.2	19.5	–	–	–	–	–	–	–
Amphibole	–	–	33.2	–	–	12.5	18.8	–	–
Magnetite	–	–	5.0	–	–	4.7	4.2	–	–
Ilmenite	–	–	0.3	–	–	1.5	1.2	–	–
Total solid added	43.1	40.1	47.4	43.4	25.5	31.0	33.6	4.4	12.8
Sum of squares of residuals	0.684	0.807	0.056	0.841	0.594	0.091	0.055	7.864	9.966

Mineral compositions from Tables 1, 2, 3, and 4; parental magma composition from Table 6

Table 8. Major and trace element modelling of the crystal fractionation process from parental magma to UZ-QGa. Estimations on water-free basis

Major elements			Trace elements						
	(a)	(b)		(c)	(d)		(c)	(d)
Plagioclase	0.127	0.461	Sc	25	22	La	17	14.1
Orthopx	0.033	0.118	Cr	19	16–46	Ce	32	29
Clinopx	0.022	0.082	Co	27	19–27	Sm	3.9	3.2
Amphibole	0.065	0.238	Ni	5	8–10	Eu	0.99	0.89
Magnetite	0.023	0.085	Rb	34	27–43	Tb	0.54	0.50
Ilmenite	0.005	0.017	Sr	292	301–317	Yb	2.1	1.7
			Zr	101	89–107			
y	0.276		Ba	378	263–323			
			Hf	2.5	2.7			
Evolved			Ta	0.32	0.35			
liquid (F)	0.724		Th	3.7	4.7			
Sum of squares of residuals	0.004							

(a) percentages of fractionated minerals and evolved liquid; y is the bulk fractionated solid.
(b) fractionated minerals normalized to 100%.
(c) calculated trace element content in the UZ-Qga according to a perfect Rayleigh fractional crystallization process.
(d) observed trace element content; the range indicates the abundance in the UZ-Qga samples, a single value indicates the abundance in the only sample analyzed for that element

magma, could be a mixture between the parental magma (52–70%) and a solid assemblage dominated by calcic amphibole; (3) the MZ-Lga could be a mixture between the parental magma (57–75%) and a solid assemblage that is plagioclase-dominated; (4) the UZ-Qga should be a mixture between the parental magma (87–95%) and plagioclase; however, their high sum of squares of residuals (Table 7) suggests that this model cannot account for the formation of the UZ-Qga.

The presence of clinopyroxene in the solid assemblage of gabbroic units generated in the second step (Table 7), seems in contrast with the crystallization of this phase in the first step. However, it must be considered that clinopyroxene acts as a seed for calcic amphibole nucleation, and hence it is involved in the solid assemblage of gabbroic units generated in the second step.

Regarding the UZ-Qga unit, an alternative hypothesis is that it may represent the evolved liquid accumulating at the top of the magma chamber during the crystallization of the parental magma (e.g. Sparks et al. 1984). This hypothesis does not contrast with the proposed model for the differentiation of the gabbroic units. In fact, in a closed system crystallization process, a solid phase accumulating, for instance, at the bottom of the magma chamber, must be balanced by a liquid phase migrating towards the top of the magma chamber in order to satisfy mass balance criteria. The hypothesis has been tested using XLFRAC (Stormer and Nicholls 1978), and the average UZ-Qga

composition can be modelled by ~ 28% crystal fractionation of plagioclase + pyroxenes + calcic amphiboles + oxides from the parental magma (Table 8). It is important to note that these phases are just the cumulus minerals occurring in the other gabbroic units.

The presence in the UZ-Qga of plagioclase with core An_{90} and patchy-zoning texture may be explained by floating of plagioclase towards the top of the magma chamber (e.g. Campbell et al. 1978), where this phase was in disequilibrium with the evolved liquid and hence developed patchy texture.

Trace element modelling

The major element differentiation of the Punta Falcone gabbroic complex can be modelled by two main processes: (1) a mixture between parental magma and minerals formed early in the crystallization sequence, which explains the formation of cumulate rocks; (2) a crystal fractionation process, which explains the formation of UZ-Qga. Therefore, trace element modelling has to be separately applied to the two different groups of rocks.

Cumulate rocks exhibit different enrichments in trace elements according to the main cumulus phase(s). The LZ-Ga and UZ-Ga are enriched in TiO_2, Sc, V, and Co (Fig. 4; Table 5) owing to the accumulation of calcic amphibole and oxides (Table 7). The MZ-Ga are enriched in Ni and Cr, and slightly in Sr and Al_2O_3 (Fig. 4; Table 5) owing to the accumulation of orthopyroxene and plagioclase, respectively (Table 7). The MZ-Lga are significantly enriched in Sr and Al_2O_3 (Fig. 4; Table 5) owing to the accumulation of plagioclase (Table 7). It is noteworthy that the absence of a positive Eu anomaly in the MZ-Lga (Fig. 5A) is probably due to crystallization under high fO_2 conditions, which considerably reduce the Kd^{Eu} of plagioclase because of the change of the oxidation state ($Eu^{2+} \rightarrow Eu^{3+}$, Irving 1978).

A quantitative estimation has been performed modifying Eq. 6. As with the major element modelling, the trace element composition of the two liquids formed during the two steps of crystallization of the gabbroic complex, has been assumed equal to that of the parental magma because the compositional difference between L_1 and L_2 is negligible and does not affect the estimations (see major element modelling). In particular, the trace element composition of the parental magma is taken from sample SP79, which has the complete set of trace elements and belongs to the three UZ-Ga samples considered representative of the parental magma on the basis of major elements.

The concentration of trace element j in the mineral phase k (Cs_k^j) is given by $Kd_k^j L^j$ (e.g. Cox et al. 1979); where Kd_k^j is the partition coefficient of trace element j for the mineral phase k, and L^j is the concentration of trace element j in the parental magma. Thus, the concentration of trace element j in a gabbroic unit (GU^j) is given by:

$$GU^j = \sum z_k Kd_k^j L^j + hL^j \quad (7)$$

or

$$GU^j = \sum D^j L^j + hL^j \quad (8)$$

where $D^j = \sum z_k Kd_k^j$, and represents the bulk distribution coefficient of trace element j according to the estimated percentages of minerals added to the parental magma to generate a gabbroic unit.

Accordingly, Eq. 8 has been applied to representative samples of the different cumulate rocks, using a subset of

Table 9. Trace element modelling of the Punta Falcone gabbroic complex differentiation

	Step I MZ-Ga				Step II LZ-Ga		MZ-Lga				UZ-Ga			
	SP 71		SP 39		SP 96		SP 77		SP 54		SP 37		SP 75	
	(a)	(b)	(a)	(b)	(a)	(b)	(a)	(b)	(a)	(b)	(a)	(b)	(a)	(b)
Sc	–	–	30	28	62	50	–	–	24	21	44	47	–	–
Cr	61	64	60	63	32	39	18	13	25	20	47	36	43	38
Co	39	36	39	37	49	57	19	20	25	25	48	56	49	65
Ni	21	21	20	22	9	10	5	11	7	8	11	9	11	10
Rb	15	10	15	10	13	25	15	25	19	33	17	14	17	17
Sr	278	296	275	311	208	225	376	387	332	345	231	243	220	244
Zr	46	53	49	71	53	63	45	80	59	79	61	58	61	61
Ba	173	177	180	189	158	157	180	220	222	246	201	213	195	218
Hf	–	–	1.2	1.3	1.3	1.8	–	–	1.4	1.6	1.5	1.6	–	–
Ta	–	–	0.18	0.20	0.28	0.20	–	–	0.20	0.29	0.25	0.15	–	–
Th	–	–	1.6	1.1	1.5	1.3	–	–	2.0	1.9	1.9	1.6	–	–
La	–	–	8.4	7.6	7.7	6.9	–	–	10.4	11.3	9.6	7.0	–	–
Ce	–	–	16	14.5	15	14	–	–	20	21	19	14	–	–
Sm	–	–	2.05	2.3	2.8	2.4	–	–	2.5	2.7	2.8	2.1	–	–
Eu	–	–	0.60	0.79	0.80	0.85	–	–	0.71	0.78	0.78	0.72	–	–
Tb	–	–	0.32	0.40	0.50	0.40	–	–	0.37	0.42	0.46	0.32	–	–
Yb	–	–	1.22	1.2	1.55	1.7	–	–	1.35	1.3	1.57	1.1	–	–
r	0.9982		0.9949		0.9904		0.9827		0.9956		0.9963		0.9953	
y err	4.4%		5.9%		6.1%		18.9%		6.4%		4.4%		6.6%	

(a) calculated values from Eq. 8, see text for explanation; (b) observed values
r: linear correlation coefficient between calculated and observed composition; y err: average error deviations of y values

trace elements, Kd values from Appendix 1, and z_k values from Table 7. The set of results is reported in Table 9. The calculated trace element contents in the representative samples match fairly well those observed, and correlation coefficients between observed and calculated compositions are significant at 95% confidence-limit error. Some lithophile elements, however, do not fit the model (e.g. Ba and Zr in sample SP77, Table 9). This fact, inasmuch as these elements are enriched in the surrounding granite, may suggest that some interaction process with the host-rock has been operative inside the gabbroic units, even though it had negligible effects on most major and trace elements.

The UZ-Qga unit exhibits smooth enrichment/depletion factors with respect to the parental magma, owing to the small range of crystal fractionation which occurred ($\sim$ 28%, Table 8). Ferromagnesian elements (Fig. 4; Table 5) are depleted because of the fractionation of pyroxenes, calcic amphibole, and magnetite. LIL and HFS elements (Fig. 4; Table 5) are enriched because they are not partitioned in the fractionating mineral assemblage, whereas Sr, REE, and Y are either slightly or not enriched because their bulk distribution coefficient in the fractionating mineral assemblage is near unity.

The trace element composition of the UZ-Qga has been calculated by a perfect Rayleigh fractional crystallization process, using the percentages of fractionated minerals from Table 5. The calculated composition of the UZ-Qga unit (Table 8) is in agreement with that observed, and supports the hypothesis that this unit could represent the evolved liquid accumulating at the top of the magma chamber during the crystallization of the parental magma. However, as in the cumulate rocks, some discrepancies do arise from the calculated composition, in particular as regards Ba (Table 8). This fact, again, is suggestive of the occurrence of interaction processes with the host-rock, affecting the composition of some lithophile elements in the crystallizing mafic magma.

In summary, major and trace element modelling give an exhaustive explanation of the differentiation of the Punta Falcone gabbroic units by the two processes discussed above. The injection of the mafic magma into the still partially molten host-granite caused the occurrence of interaction processes which do not seem to have greatly affected the bulk chemical composition of the interior zone of the gabbroic complex, but only slightly modified the composition of some lithophile elements.

Genesis of the Interaction Zone

The envelope of fine-grained rocks enclosing and grading into the coarser inner parts of the Punta Falcone gabbroic complex cannot be envisaged as a classical chilled margin, owing to their high petrographical and chemical (Table 5) variability, in such a narrow outcrop surface (Fig. 1). In addition, the estimation of crystallization temperature on amphibole-plagioclase pairs in the IZ ($\sim$ 800°C) is too low to indicate quenching of a high-alumina basalt (e.g. Baker and Eggler 1983).

A possibility is that the IZ rocks were formed by simple fractional crystallization of the Punta Falcone mafic magma. This process alone, however, is not thermodynamically likely because the energy budget of mafic magmas permits considerable digestion of granite magmas (e.g. Bowen 1928; McBirney 1979; DePaolo 1981; Huppert and Sparks 1985).

Another possibility is that the IZ may resemble the so-called *thermal boundary layer* (Huppert and Sparks 1988). According to these authors, the thermal boundary layer is a dynamical region along the interface between co-existing mafic and granite magmas, where there is a very steep temperature gradient. Then, the IZ may represent the Punta Falcone mafic magma cooling and crystallizing more rapidly along contacts with the granite magma than in the interior zone. Hybridization processes are expected to be operative in the thermal boundary layer (Huppert and Sparks 1988), even though simple mixing processes are ruled out on the basis of thermodynamic constraints, owing to temperature and viscosity difference between mafic and acid magmas (e.g. Campbell and Turner 1985, 1986). A simple two end-member mixing process fails in fact to explain the geochemical features of the IZ rocks, inasmuch as most trace elements, in particular HFSE and REE, have higher abundances than in the mafic and acid end-members (Fig. 4; Table 5). Hybridization processes could have also occurred by contamination of the crystallizing mafic magma by the granite magma. Thus, the leading process responsible for the genesis of the IZ rocks could have been a *contamination plus fractional crystallization* (CFC) process, as it has been already suggested to account for interaction processes between acid and mafic magmas (Poli and Tommasini 1991b).

The composition of the contaminant magma is assumed to be that of the host-granite, even though contamination processes by crustal rocks during the uprising of the mafic magma from the mantle through the lower crust cannot be ruled out. In contrast, the composition of the mafic magma is not confined to that of the parental magma of the gabbroic complex, but also to each crystal-mush magma which formed the different units. In fact, the IZ was a dynamical region which evolved continuously while the mafic magma experienced differentiation. Thus, the composition of the magma along the interface with the host-granite was neither constant nor homogeneous, because it changed in time and space during differentiation of the mafic magma. Accordingly, the CFC process has been tested for a subset of trace elements using the AFC equation by DePaolo (1981), and representative samples of each gabbroic unit as starting mafic material.

The percentages of fractionating phases cannot be directly determined, but geochemical data allow some rough estimates. The depletion in MgO, FeO, Ni, Sc, V, Cr, and Sr (Fig. 4; Table 5), the increase of the negative Eu anomaly and the decrease of the $(Tb/Yb)_n$ ratios (Fig. 5B and Table 5) with evolution, suggest fractionation of plagioclase, pyroxenes, amphibole, and oxides. However, the increase of REE content (Fig. 5B), in particular HREE, excludes amphibole as the main fractionating phase owing to its high Kd for HREE (see Appendix 1). Also, the increase of the absolute Eu abundance (Table 5) indicates an incompatible behaviour for this element, i.e. the fractionating plagioclase has a low Kd^{Eu}.

The behaviour of trace elements in each IZ rock can be modelled by generating, at constant R = 0.3 (rate of con-

tamination over rate of crystallization), a family of liquid lines of descent starting from different mafic materials, and varying the range of residual liquid (F) from 0.9 to 0.3. The fractionating mineral assemblage which exhibits the best fitting result of the CFC process consists of plagioclase (~ 58%) + clinopyroxene (~ 10%) + amphibole (~ 20%) + oxides (~ 12%).

Binary inter-elemental diagrams are reported in Fig. 7 to illustrate the CFC process. Among the family of the modelled liquid lines of descent, only two lines, using the trace element composition of SP80 (UZ-Ga) and SP54 (MZ-Lga), are reported as an example, because these two lines encompass almost all the spectrum of the compositional variation of the IZ rocks.

The only sample that does not fit the CFC process is the most evolved IZ rock (SP32), in particular its Ba and Eu contents (Fig. 7), and probably K_2O and P_2O_5 contents, as they have the same behaviour as Ba (Fig. 4). A plausible explanation for this discrepancy may be that in the latest stages of crystallization (F = 0.3–0.1) the amount of fractionating plagioclase increased and K-feldspar + small amounts of apatite entered the fractionating

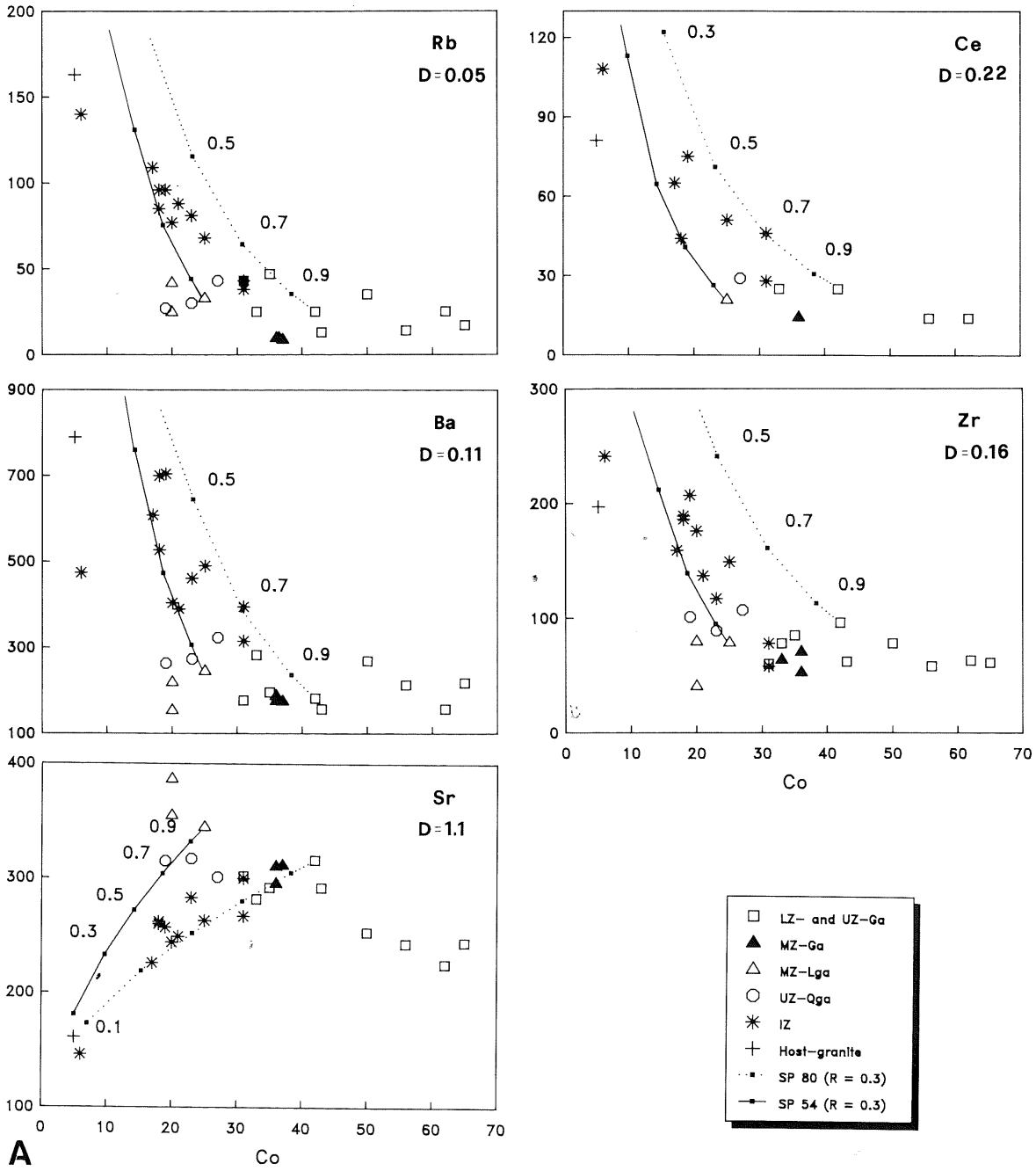

Fig. 7A, B. Trace element modelling of the CFC process responsible for the genesis of the IZ. The liquid lines of descent for R = 0.3 are reported for two samples. D, bulk distribution coefficient; figures indicate the values of residual liquid (F)

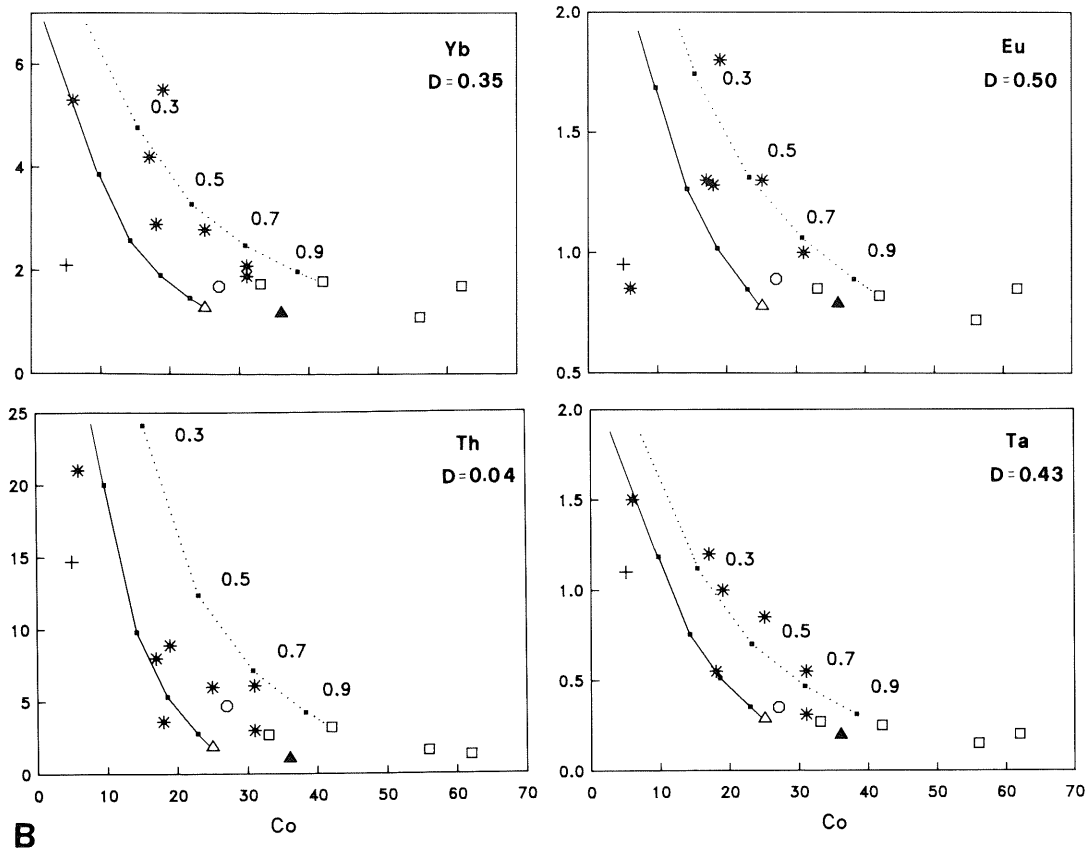

Fig. 7. (continued)

mineral assemblage. Then, Ba, Eu, K_2O, and P_2O_5 no longer behaved as incompatible elements, and consequently have been depleted in the residual liquid.

It is noteworthy that the CFC process can also explain the different compositional trend exhibited by calcic amphibole of the IZ with respect to those of the gabbroic units (Fig. 3). The contamination by the granite magma resulted in the enrichment of lithophile elements in the evolving mafic magma, and hence the tschermakite-type substitution could be replaced by the edenite-type ($Si \leftrightarrow Na + Al^{IV}$).

The proposed CFC process takes into account contamination by the bulk granite magma. However, it is important to note that additional complications can arise due to selective contamination (e.g. Watson 1982; Watson and Jurewicz 1984; Johnston and Wyllie 1988). In particular, selective contamination by K_2O could have stabilized the crystallization of biotite in the mafic magma. This phase could potentially serve as a sink for various lithophile elements (e.g. Rb and Ba) and thereby promote further exchange of these elements between the two magmas. This process could explain the observed discrepancies in the trace element modelling of some lithophile elements. The present geochemical data of the IZ rocks, however, do not allow this possibility to be considered in detail.

Physical model for the evolution of the gabbroic complex

The differentiation of the Punta Falcone gabbroic complex can be accounted for by three main processes on the basis of petrographic data and major and trace element modelling. The sequence of the occurrence of these processes on a time-space scale is the subject of the following section.

The first topic to be evaluated is the depth at which the high-alumina basalt intruded the host-granite magma. A possibility is that the mafic magma intruded the acid magma during the emplacement of the acid magma in middle crustal levels (10–12 km, Poli and Tommasini 1991a), and then it was passively carried up. However, estimated settling velocities for the mafic magma are too high for this hypothesis to be reasonable. Another possibility is that the mafic magma rose from mantle through lower crust, and intruded the host-granite magma in middle crustal levels. Olivine fractionation could have occurred during its ascent, permitting the development of the evolved geochemical features which characterize the Punta Falcone parental magma. This hypothesis is more likely because the hornblende geobarometer yields the same crystallization pressures as the host-granite (3–4 kbar), and also, the low Al_2O_3 content of pyroxenes suggests low pressures of crystallization.

Another topic concerns the physical state of both granite and mafic magma when they came in contact. The granite magma should have been near or below the rheologically critical melt percentage (RCMP, Arzi 1978), to prevent sinking of the mafic magma. In turn, the mafic magma should have been almost completely liquid to allow buoyancy through the lower crust. However, the mafic magma might carry some plagioclase crystals in suspension, owing to their lower density than basaltic magmas. This hypothesis is suggested by the estimated Al_2O_3 content of the parental magma ($\sim$ 19%), and is supported by experimental studies (e.g. Campbell et al. 1978), and by the fact that the Punta Falcone parental magma was saturated with plagioclase.

Thus, the Punta Falcone parental magma can be envisaged as an evolved high-alumina basalt (1100–1150°C) injected into an almost totally crystallized granite magma (670–700°C) in middle crustal levels.

Processes which occurred in its interior zone have been substantially different from those which occurred in its marginal interaction zone. As an attempt to reach equilibrium, the mafic magma overcooled along contacts with the granite magma, which, in turn, was superheated by the latent heat of crystallization of the mafic magma. However, the temperature contrast was not sufficient to permit the formation of a chilled margin (e.g. Huppert and Sparks 1988), even though the envelope of the "frozen" IZ rocks thermally isolated the interior of the chamber, permitting extensive growth of crystal nuclei.

The crystallization of the interior of the gabbroic complex can be modelled by two steps during which the different minerals nucleated and grew in-situ on the floor and walls of the chamber (see Major element modelling, above). The first step concerned the anhydrous crystallization of plagioclase and pyroxenes, whereas the second step concerned the hydrous crystallization of plagioclase, calcic amphiboles and oxides. Floating of plagioclase towards the top of the magma chamber was an operative mechanism, and permitted the accumulation of the denser liquid at the bottom (Fig. 8A). Subsequently, compaction phenomena and convective fractionation processes allowed the development of the pile of cumulus crystals with their trapped liquid, and the migration of part of this evolved liquid towards the top of the magma chamber to form the UZ-Qga (Campbell 1978; McBirney and Noyes 1979; Sparks et al. 1984). Accordingly, the gabbroic complex acquired a sub-horizontal stratified structure (Fig. 8B).

Contemporaneously with the differentiation of the interior zone, the marginal interaction zone of the gabbroic complex experienced both chemical and physical processes. Chemical processes determined the evolution of the marginal interaction zone by crystal fractionation of plagioclase + clinopyroxene + calcic amphibole + oxides, and contamination by the acid magma (CFC process).

It is noteworthy that this kind of process may have been slightly operative even inside the interior zone, as it is suggested by discrepancies arising from modelling the behaviour of some lithophile elements in the gabbroic units.

Physical processes were closely related to the thermodynamic instability of this marginal interaction zone. In fact, an increase of melt fraction of the granite magma along contacts did occur, owing to the latent heat of crystallization released by the mafic magma (see also Huppert and Sparks 1988). This thermodynamic instability resulted in mingling (i.e. mechanical) processes and back-veining phenomena. The effective result was the development of dense interdigitations of granite veins at contacts with the IZ rocks (Fig. 8A). In addition, the melt

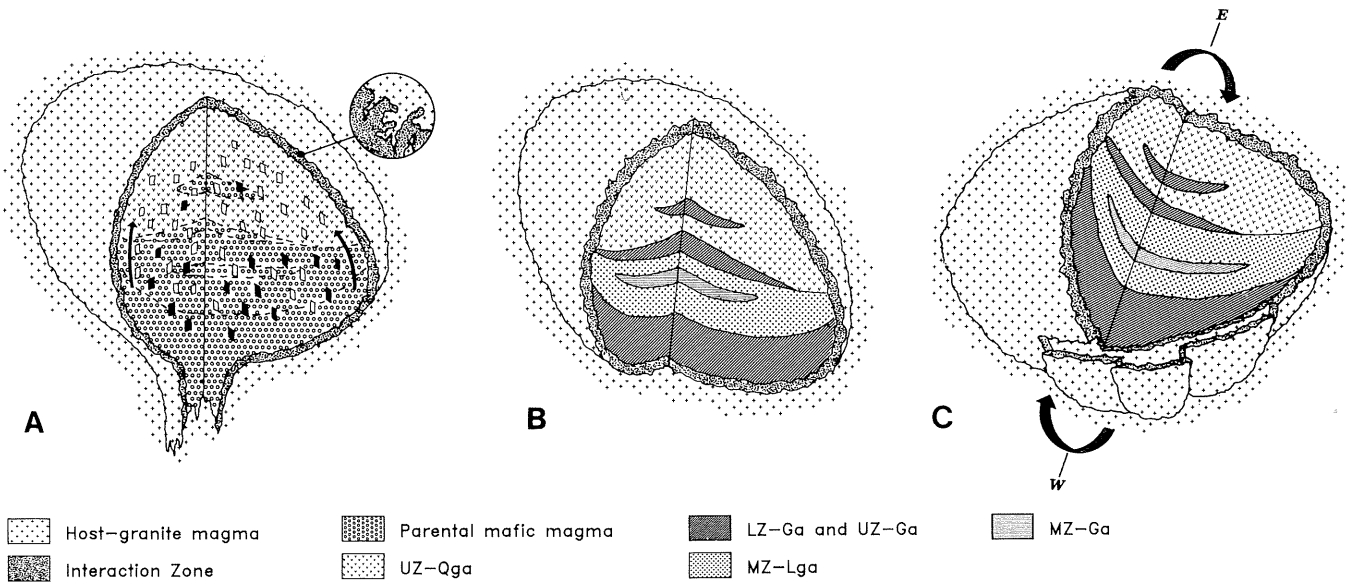

Fig. 8A–C. Schematic cartoons showing the differentiation history of the Punta Falcone gabbroic complex (see text for explanation). *Closed parallelograms*, mafic phases; *open parallelograms*, plagioclase

fraction of granite magma immediately close to contacts rose above the RCMP (Arzi 1978), and caused the occurrence of a differential sinking and an almost 90° tilting of the magma chamber (Fig. 8C). This movement resulted in the development of the sub-vertical structure of the gabbroic complex (Fig. 1), as well as a local shear zone which caused the detachment of some parts of IZ, forming the dike-like fragments outcropping at the northwestern edge of the complex (Fig. 1 and Fig. 8C). Finally, the occasional occurrence of angular fragments of the different gabbroic units in the IZ rocks could also be explained by the almost 90° tilting which resulted in disruption of the already solidified parts of the gabbroic complex.

Appendix 1

Set of partition coefficients

	Pl	Hb	Opx	Cpx	Ox
Sc	0	4.2	2	2.5	1
Cr	0	1.59	8	10	1
Co	0	1.8	3	2	6.6
Ni	0	1	10	6	4
Rb	0.07	0.05	0.02	0.02	0
Sr	1.8	0.23	0.03	0.08	0
Zr	0.02	0.4	0.1	0.25	0.4
Ba	0.16	0.09	0.02	0.02	0
Hf	0.01	0.4	0.1	0.25	0.4
Ta	0.03	1.3	0.35	0.3	1
Th	0.01	0.15	0	0	0
La	0.21	0.14	0.03	0.14	0.22
Ce	0.2	0.25	0.05	0.25	0.2
Sm	0.11	1	0.1	0.75	0.3
Eu	0.31	1.1	0.12	0.8	0.25
Tb	0.08	1.5	0.3	1.1	0.3
Yb	0.05	1	0.46	0.9	0.25

Source of data: the compilation by Gill (1981)

Acknowledgements. We are particularly grateful to P. Manetti, C. Ghezzo, G. Piccardo, L. Francalanci, and S. Feldstein for critical comments to the first draft of the manuscript. The manuscript also benefitted from constructive comments by the reviewers P. Michael and R. A. Wiebe. We wish to thank D. Chiocchini and M.L. Todaro for technical assistance. This work was supported by M.U.R.S.T. of Italy (grants 40% and 60%).

References

Arzi AA (1978) Critical phenomena in the rheology of partially melted rocks. Tectonophysics 44:173–184

Baker DR, Eggler DH (1983) Fractionation paths of Atka (Aleutians) high-alumina basalts: constraints from phase relations. J Volcanol Geotherm Res 18:387–404

Bralia A, Ghezzo C, Guasparri G, Sabatini G (1982) Aspetti genetici del batolite Sardo-Corso. Rend Soc Ital Mineral Petrol 38:701–764

Blundy JD, Holland TJB (1990) Calcic amphibole equilibria and a new amphibole-plagioclase geothermometer. Contrib Mineral Petrol 104:208–224

Bowen NL (1928) The evolution of the igneous rocks. Princeton University Press, Princeton, N.J.

Brooks CK, Nielsen TFD (1990) The differentiation of the Skaergaard intrusion. A discussion of Hunter and Sparks 1987. Contrib Mineral Petrol 104:244–247

Campbell IH (1978) Some problems with cumulus theory. Lithos 11:311–323

Campbell IH, Turner JS (1985) Turbulent mixing between fluids with different viscosities. Nature 313:39–42

Campbell IH, Turner JS (1986) The influence of viscosity on fountains in magma chamber. J Petrol 27:1–30

Campbell IH, Roeder PL, Dixon JM (1978) Plagioclase buoyancy in basaltic liquids as determined with a centrifuge furnace. Contrib Mineral Petrol 67:369–377

Colby JW (1971) Magic IV, a computer programme for quantitative electron microprobe analysis. Bell Telephone Lab, Allentown

Cox KG, Bell JD, Pankhurst RJ (1979) The interpretation of igneous rocks. George Allen and Unwin, London

DePaolo DJ (1981) Trace element and isotopic effects of combined wall-rock assimilation and fractional crystallization. Earth Planet Sci Lett 53:189–202

Franzini M, Leoni L (1972) A full matrix correction in X-ray fluorescence analysis of rock samples. Atti Soc Toscana Sci Nat Ser A79:7–22

Gill JB (1981) Orogenic andesites and plate tectonics. Springer, Berlin

Green TH, Ringwood AE (1968) Genesis of the calc-alkaline igneous rock suite. Contrib Mineral Petrol 18:105–162

Hammarstrom JM, Zen E (1986) Aluminum in hornblende: an empirical igneous geobarometer. Am Mineral 71:1297–1313

Haskin LA, Frey FA, Schmitt RA, Smith RH (1966) Meteoric, solar and terrestrial rare-earth distributions. Phys Chem Earth 7:167–321

Holloway JR, Burnham CW (1972) Melting relations of basalt with equilibrium water pressure less than total pressure. J Petrol 13:1–29

Hughes CJ (1982) Igneous petrology. Elsevier, New York

Hunter RH, Sparks RSJ (1987) The differentiation of the Skaergaard intrusion. Contrib Mineral Petrol 95:451–461

Hunter RH, Sparks RSJ (1990) The differentiation of the Skaergaard intrusion. Reply to McBirney and Naslund 1990. Contrib Mineral Petrol 104:248–254

Huppert HE, Sparks RSJ (1985) Cooling and contamination of mafic and ultramafic magmas during ascent through continental crust. Earth Planet Sci Lett 74:371–386

Huppert HE, Sparks RSJ (1988) The generation of granitic magmas by intrusion of basalt into continental crust. J Petrol 29:599–624

Irvine TN (1979) Rocks whose composition is determined by crystal accumulation and sorting. In: Yoder HS (ed) The evolution of igneous rocks. Princeton University Press, Princeton, N.J., pp 245–306

Irvine TN (1980) Magmatic infiltration metasomatism, double-diffusive fractional crystallization, and adcumulus growth in the Muskox intrusion and other layered intrusions. In: Hargraves RB (ed) Physics of Magmatic Processes. Princeton University Press, Princeton, pp 325–384

Irving AJ (1978) A review of experimental studies of crystal/liquid trace element partitioning. Geochim Cosmochim Acta 42:743–770

Johnston AD, Wyllie PJ (1988) Interaction of granitic and basic magmas: experimental observations on contamination processes at 10 kbar with H_2O. Contrib Mineral Petrol 98:352–362

Kaye MJ (1965) X-ray fluorescence determinations of several trace elements in some standard geochemical samples. Geochim Cosmochim Acta 29:139–142

Klewin KW (1990) Petrology of the Proterozoic Potato River layered intrusion, Northern Wisconsin, USA. J Petrol 31:1115–1139

Leake BE (1978) Nomenclature of amphiboles. Am Mineral 63:1023–1052

McBirney AR (1979) Effects of assimilation. In: HS Yoder Jr (ed) The evolution of the igneous rocks. Princeton University Press, Princeton, pp 307–338

McBirney AR, Naslund HR (1990) The differentiation of the Skaergaard intrusion. A discussion of Hunter and Sparks 1987. Contrib Mineral Petrol 104:235–240

McBirney AR, Noyes RM (1979) Crystallization and layering of the Skaergaard intrusion. J Petrol 20:454–487

Morse SA (1990) The differentiation of the Skaergaard intrusion. A discussion of Hunter and Sparks 1987. Contrib Mineral Petrol 104:240–244

Nakajima Y, Ribbe PH (1981) Texture and structural interpretation of the alteration of pyroxene to other biopyroboles. Contrib Mineral Petrol 78:230–239

Orsini JB (1980) Le Batholithe Corse-Sarde: Anatomie d'un batholite hercynien. PhD Thesis Universite' de Aix-Marseille

Pearce JA (1982) Trace element characteristics of lavas from destructive plate boundaries In: Thorpe RS (ed) Andesites: orogenic andesites and related rocks. John Wiley, Chichester, pp 525–548

Pearce JA, Cann JR (1973) Tectonic setting of basic volcanic rocks determined using trace element analysis. Earth Planet Sci Lett 19:290–300

Perfit MR, Gust DA, Bence AE, Arculus RJ, Taylor SR (1980) Chemical characteristics of island arc basalts: implications for mantle sources. Chem Geol 30:227–256

Poli G, Manetti P, Peccerillo A, Cecchi A (1977) Determinazione di alcuni elementi del gruppo delle terre rare in rocce silicatiche per attivazione neutronica. Rend Soc Ital Mineral Petrol 33:755–763

Poli G, Ghezzo C, Conticelli S (1989) Geochemistry of granitic rocks from the Hercynian Sardinia-Corsica Batholith: Implication for magma genesis. Lithos 23:247–266

Poli G, Tommasini S (1991a) A geochemical approach to the evolution of granitic plutons: a case study, the acid intrusions of Punta Falcone (Northern Sardinia, Italy). Chem Geol 92:87–105

Poli G, Tommasini S (1991b) Model for the origin and significance of microgranular enclaves in calc-alkaline granitoids. J Petrol 32:657–666

Ragland PR, Butler JR (1972) Crystallization of the West Farrington pluton, North Carolina, USA. J Petrol 13:381–404

Sparks RSJ, Huppert HE, Turner JS (1984) The fluid dinamics of evolving magma chambers. Phil Trans R Soc London A310:511–534

Stormer JC, Nicholls J (1978) XLFRAC a programme for interactive testing of magmatic differentiation models. Computers Geosci 4:143–159

Sun SS (1980) Lead isotopic study of young volcanic rocks from mid-ocean ridges, ocean islands and island arcs. Phil Trans R Soc London A297:409–445

Wager LR, Brown GM (1967) Layered igneous rocks. Freeman, San Francisco

Watson BE (1982) Basalt contamination by continental crust: some experiments and models. Contrib Mineral Petrol 80:73–87

Watson BE, Jurewicz SR (1984) Behaviour of alakalies during diffusive interaction of granitic xenoliths with basaltic magma. J Geol 92:121–131

Wood DA, Joron JL, Treuil M (1979) A re-appraisal of the use of trace elements to classify and discriminate between magma series erupted in different tectonic settings. Earth Planet Sci Lett 45:326–336

Editorial responsibility: T.L. Grove